The 14-3-3 Protein Affects the Conformation of the Regulatory Domain of Human Tyrosine Hydroxylase†

Veronika Obsilova,‡ Eliska Nedbalkova,‡,§ Jan Silhan,‡,§ Evzen Boura,‡,§ Petr Herman,|| Jaroslav Vecer,|| Miroslav Sulc,⊥ Jan Teisinger,‡ Fred Dyda,# and Tomas Obsil*,‡,§

Department of Physical and Macromolecular Chemistry, Faculty of Science, Charles University, 12843 Prague, Czech Republic, Institute of Physiology, Academy of Sciences of the Czech Republic, 14220 Prague, Czech Republic, Faculty of Mathematics and Physics, Institute of Physics, Charles University, 12116 Prague, Czech Republic, Institute of Microbiology, Academy of Sciences of the Czech Republic, 14220 Prague, Czech Republic, Department of Biochemistry, Faculty of Science, Charles University, 12843 Prague, Czech Republic, and Laboratory of Molecular Biology, National Institute of Diabetes and Digestive and Kidney Diseases, National Institutes of Health, Bethesda, Maryland 20892

Received September 26, 2007; Revised Manuscript Received November 21, 2007

ABSTRACT: Tyrosine hydroxylase (TH) catalyzes the first step in the biosynthesis of catecholamines. Regulation of TH enzyme activity is controlled through the posttranslational modification of its regulatory domain. The regulatory domain of TH can be phosphorylated at four serines (8, 19, 31, and 40) by a variety of protein kinases. Phosphorylation of Ser[19] does not by itself increase TH activity but induces its binding to the 14-3-3 protein. That leads to the enhancement of TH activity with a still not fully understood mechanism. The main goal of this work was to investigate whether the 14-3-3 protein binding affects the conformation of the regulatory domain of human TH isoform 1 (TH1R). Site-directed mutagenesis was used to generate five single-tryptophan mutants of TH1R with the Trp residue located at five different positions within the domain (positions 14, 34, 73, 103, and 131). Time-resolved tryptophan fluorescence measurements revealed that phosphorylation of Ser[19] and Ser[40] does not itself induce any significant structural changes in regions surrounding inserted tryptophans. On the other hand, the interaction between the 14-3-3 protein and phosphorylated TH1R decreases the solvent exposure of tryptophan residues at positions 14 and 34 and induces distinct structural change in the vicinity of Trp[73]. The 14-3-3 protein binding also reduces the sensitivity of phosphorylated TH1R to proteolysis by protecting its N-terminal part (first 33 residues). Circular dichroism measurements showed that TH1R is an unstructured protein with a low content of secondary structure and that neither phosphorylation nor the 14-3-3 protein binding changes its secondary structure.

Tyrosine hydroxylase (TH,[1] EC 1.14.16.2) catalyzes the first step in the biosynthesis of catecholamines, and its activity is controlled by multiple mechanisms, including feedback inhibition by catecholamines, allosteric activation by heparin, phospholipids, and RNA, and activation by protein phosphorylation (*1*−*3*). The N-terminal regulatory domain of TH consists of 160−190 amino acid residues (in human isoforms) and can be removed without a significant decrease in catalytic activity (*4*). The regulatory domain can be phosphorylated at four serine residues, Ser[8], Ser[19], Ser[31], and Ser[40], in vitro, in situ, and in vivo (Figure 1A) (*2*, *3*, *5*−*7*). Among these, the effects of Ser[19] and Ser[40] phosphorylation are the best characterized. Residue Ser[40] can be phosphorylated by a number of protein kinases, and its phosphorylation by cyclic AMP-dependent protein kinase (PKA) induces the most potent activation of TH (*8*−*11*). It has been proposed that phosphorylation of Ser[40] alters the conformation of the regulatory domain and its interaction with the catalytic domain. Phosphorylation of Ser[40] is known to increase the sensitivity to proteolysis in its surrounding, while dopamine binding has the opposite effect, suggesting that there is a link between the conformation of the regulatory

† This work was funded by Grant KJB500110601 of the Grant Agency of the Academy of Sciences of the Czech Republic, by Grant 204/06/0565 of the Grant Agency of the Czech Republic, by Grant B/CH/331/2005 of the Grant Agency of Charles University, by Research Projects MSM0021620857 and MSM0021620835 and Centre of Neurosciences LC554 of the Ministry of Education, Youth, and Sports of the Czech Republic, and by Research Project AV0Z50110509 of the Academy of Sciences of the Czech Republic.

* To whom correspondence should be addressed: Faculty of Science, Charles University, 12843 Prague, Czech Republic. Telephone: +420-221951303. Fax: +420-224919752. E-mail: obsil@natur.cuni.cz.

‡ Institute of Physiology, Academy of Sciences of the Czech Republic.

§ Department of Physical and Macromolecular Chemistry, Faculty of Science, Charles University.

|| Faculty of Mathematics and Physics, Institute of Physics, Charles University.

⊥ Institute of Microbiology, Academy of Sciences of the Czech Republic, and Department of Biochemistry, Faculty of Science, Charles University.

National Institutes of Health.

[1] Abbreviations: CD, circular dichroism; MALDI-TOF, matrix-assisted laser desorption ionization time of flight; MEM, maximum entropy method; MCP, multichannel plate photomultiplier; PKA, protein kinase A; PSD, post-source decay; SVD, singular-value decomposition; TH, tyrosine hydroxylase; TH1R, regulatory domain of tyrosine hydroxylase (isoform 1); dpTH1R, doubly phosphorylated (at Ser[19] and Ser[40]) regulatory domain of tyrosine hydroxylase (isoform 1); WT, wild-type.

10.1021/bi7019468 CCC: $40.75
Published on Web 01/09/2008

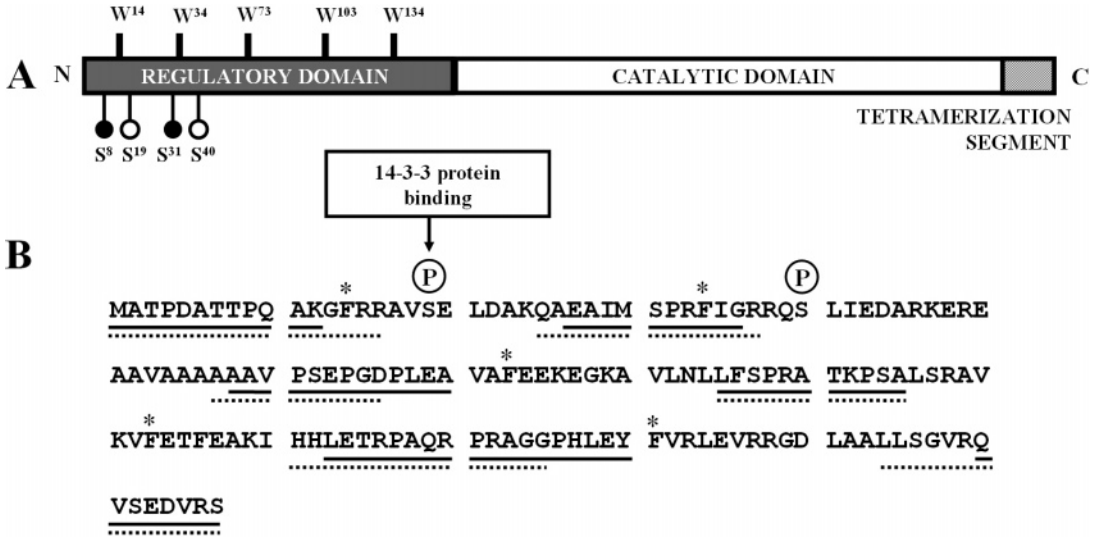

FIGURE 1: (A) Diagram of tyrosine hydroxylase primary structure. Relative positions of the phosphorylation sites and inserted tryptophans within the regulatory domain are shown. (B) Amino acid sequence of human TH1R with the theoretical prediction of disordered regions. Prediction was calculated using either loops/coils definitions (underlined with a solid line) or hot-loops definitions (underlined with a dotted line) (*44*−*46*). Phenylalanine residues that were replaced with tryptophan residues are labeled with asterisks. Phosphorylation sites Ser^{19} and Ser^{40} are indicated with a circled P.

domain and the enzyme activity (*12*). It has been proposed that the hydroxyl group of Ser^{40} contributes to the stabilization of the catecholamine-bound inhibited form of TH (*8*). Phosphorylation of Ser^{40} probably induces a conformational change of the regulatory domain, thus permitting easier dissociation of catecholamine and activation of TH (*11*, *13*−*15*).

In contrast to phosphorylation at Ser^{40}, the activation of TH through the phosphorylation of Ser^{19} requires the presence of regulatory 14-3-3 protein (*16*−*19*). The 14-3-3 proteins are involved in many biologically important processes, such as cell cycle control, apoptosis, and oncogenesis (*20*, *21*). The main feature of 14-3-3 proteins is their ability to bind to other proteins in a phosphorylation-dependent manner. 14-3-3 proteins recognize a motif containing either a phosphorylated serine (pS) or a phosphorylated threonine (pT) residue, which is present in most known 14-3-3 binding partners (*22*). Two optimal 14-3-3 binding motifs, RSXpSXP and RXY/FXpSXP, have been identified using oriented peptide library screening approaches (*23*, *24*). The regulatory domain of TH contains two similar sequences around residues Ser^{19} and Ser^{40} (Figure 1B). Detailed analysis of interactions between TH and different 14-3-3 protein isoforms confirmed that phosphorylation of Ser^{19} is required for stable association of human TH isoform 1 with the bovine 14-3-3ζ isoform (*25*). On the other hand, Kleppe at al. (*25*) also showed that the yeast 14-3-3 protein isoform (BMH1) can bind with high affinity to all four human TH isoforms phosphorylated only at Ser^{40}. The reason why yeast but not mammalian 14-3-3 protein isoforms bind to TH phosphorylated only at Ser^{40} is unknown.

The role of 14-3-3 protein in the regulation of TH activity is still unclear. While one study found that the 14-3-3 protein binding to TH phosphorylated at Ser^{19} increased V_{max} 3-fold (*26*), other studies observed no 14-3-3 protein-dependent enhancement of TH activity (*27*, *28*). It has also been suggested that 14-3-3 protein might protect the proteolytically very sensitive phosphorylated regulatory domain of TH and/or slow dephosphorylation of phosphorylated Ser^{19} and Ser^{40} (*25*, *26*). The phosphorylation status of the regulatory domain seems to be important for the overall stability of TH because it has been shown that the multiphosphorylated form of TH is more stable than the singly phosphorylated and unphosphorylated forms, regardless of phosphorylation sites (*13*, *26*, *29*). Since 14-3-3 proteins are known to modulate the structure of their binding partners (*30*−*32*), it is reasonable to speculate that the 14-3-3 protein changes the structure of the phosphorylated regulatory domain of TH, thus making it less sensitive to proteolysis and/or dephosphorylation.

The main goal of this work was to investigate whether 14-3-3ζ protein binding affects the conformation of the regulatory domain of human TH isoform 1 (denoted as TH1R) phosphorylated at both Ser^{19} and Ser^{40}. Site-directed mutagenesis was used to generate five single-tryptophan mutants with the tryptophan residue located at different positions within the regulatory domain (positions 14, 34, 73, 103, and 131). Time-resolved tryptophan fluorescence intensity decays revealed that phosphorylation of Ser^{19} and Ser^{40} by itself does not induce significant conformational changes in the regions surrounding inserted tryptophans. On the other hand, the interaction between the 14-3-3 protein and phosphorylated TH1R decreases the solvent exposure of tryptophan residues at positions 14 and 34 and induces distinct structural change in the vicinity of Trp^{73}. The 14-3-3ζ protein binding also reduces the sensitivity of phosphorylated TH1R to proteolysis by protecting its N-terminal part (first 33 residues). Circular dichroism measurements showed that TH1R is an unstructured protein with a low content of secondary structure and that neither phosphorylation nor 14-3-3 protein binding changes its secondary structure.

MATERIALS AND METHODS

Expression, Purification, and Phosphorylation of TH1R. The original plasmid containing cDNA of human TH1R (Met^1−Ser^{157} sequence subcloned in pET-23d) was a kind gift of S. C. Daubner (Department of Biochemistry and

Biophysics, Texas A&M University, College Station, TX). To introduce a His tag at the N-terminus of the polypeptide, the cDNA encoding TH1R ($Met^{1}-Ser^{157}$) was ligated into pET-15b (Novagen) using the NdeI and BamHI sites. The entire coding region was checked by sequencing. Since TH1R contains several cryptic thrombin cleavage sites, the thrombin cleavage site of the pET-15b plasmid (sequence SGLVPRGS) was mutated to a TEV cleavage site (sequence ENLYFQGS) using the QuickChange kit (Stratagene). All mutants of TH1R were generated using a similar approach, and their sequences were checked by sequencing. TH1R was expressed as six-His-tag fusion proteins by isopropyl 1-thio-β-D-galactopyranoside induction for 12 h at 30 °C and purified from *Escherichia coli* BL21(DE3) cells using Chelating-Sepharose Fast Flow (Amersham Biosciences) according to the standard protocol. The six-His tag was removed by incubation (1 h at 30 °C) with TEV protease (Invitrogen). Eluted protein was dialyzed against buffer [50 mM sodium citrate (pH 6.0), 2 mM EDTA, and 1 mM DTT] and purified using cation exchange chromatography on a SP-Sepharose column (Amersham Biosciences). The protein was eluted using a linear gradient of NaCl (from 50 to 1000 mM). Fractions containing TH1R were dialyzed against buffer containing 20 mM Tris (pH 7.5), 150 mM NaCl, 1 mM EDTA, and 10% (v/w) glycerol. The purified TH1R was then phosphorylated by incubation with 60 units of PKA (Promega) per milligram of recombinant protein for 2 h at 30 °C in the presence of 20 mM magnesium chloride and 0.75 mM ATP. After the phosphorylation, the TH1R was repurified using cation-exchange chromatography as mentioned above. Eluted proteins were finally dialyzed against buffer containing 20 mM Tris (pH 7.5), 150 mM NaCl, 1 mM EDTA, and 10% (w/v) glycerol. The completeness of the phosphorylation reaction was checked using MALDI-TOF mass spectrometry. Tryptophan mutants of TH1R were purified using the same approach, but all buffers contained 0.01% (v/v) Tergitol NP-40 (Sigma).

Expression and Purification of 14-3-3ζ Protein. Both human 14-3-3ζ protein (WT) and its mutant version containing no tryptophan residues (mutations Trp^{59}Phe and Trp^{228}-Phe, denoted as 14-3-3ζnoW) were prepared as described previously (*33*).

Steady-State Fluorescence Measurements and Tryptophan Fluorescence Quenching Experiments. All steady-state fluorescence measurements were performed at 23 °C on an ISS PC1 Photon counting spectrofluorometer, using a 1 nm bandpass on both the excitation and emission monochromators. Proteins (4 μM TH1R and 10 μM 14-3-3ζnoW) were dissolved in 20 mM Tris-HCl buffer (pH 7.5) containing 150 mM NaCl, 1 mM EDTA, 0.01% (v/v) Tergitol NP-40, 1 mM 2-mercaptoethanol, and 10% (w/v) glycerol. Stern−Volmer plots were constructed by using the changes in fluorescence intensity at 340 nm (with excitation at 295 nm). To take into account both collisional and static quenching processes, the Stern−Volmer plots were fitted to the following equation (*34*):

$$\frac{F_0}{F} = (1 + K_{SV}[Q])e^{V[Q]} \quad (1)$$

where F_0 is the fluorescence intensity in the absence of acrylamide, F is the fluorescence intensity of the sample in the presence of a concentration [Q] of acrylamide, K_{SV} is the Stern−Volmer constant, and V is the static quenching constant. The Stern−Volmer constant K_{SV} is equal to $\tau_{mean}k_q$, where k_q is the bimolecular rate constant for quenching and τ_{mean} is a mean fluorescence lifetime of the tryptophan in the absence of a quencher. Corrections for the inner filter effect were performed according to the following equation (*35*):

$$F_C = F \,\mathrm{antilog}[(A_{ex} + A_{em})/2] \quad (2)$$

where F_C is the corrected fluorescence intensity, F is the measured fluorescence intensity, and A_{ex} and A_{em} are sample absorbances at the excitation and emission wavelength, respectively.

Time-Resolved Fluorescence Experiments. Fluorescence experiments were measured on a time-correlated single-photon counting instrument with a pulsed UV-LED excitation (PicoQuant, PLS 295-10) and a cooled MCP-PMT (Hamamatsu, R3809U-50) detector. Subnanosecond excitation pulses with a repetition rate of 10 MHz and a half-width of 300 ps were generated at 295 nm. The LED emission was cleaned up by a custom-made bandpass filter. The fluorescence signal was isolated by a monochromator at 355 nm with a slit width of 15 nm. A color glass filter (Zeiss, UG1) placed in front of the input slit enhanced suppression of scattered light. All time-resolved emission data were acquired under the "magic angle" conditions when the intensity decay is independent of rotational diffusion of the chromophore. Therefore, it provides unbiased information about lifetimes. The decays were typically acquired in 512 channels with a time scale of 100 ps per channel, until a peak count of 10^5 was reached. Samples were placed in a thermostatic holder, and all experiments were performed at 22 °C in buffer containing 20 mM Tris-HCl buffer (pH 7.5), 150 mM NaCl, 1 mM EDTA, 0.01% (v/v) Tergitol NP-40, 1 mM 2-mercaptoethanol, and 10% (w/v) glycerol. The concentration of TH1R (single-tryptophan mutants) was 10 μM, and the 14-3-3ζnoW concentration was 20 μM.

Fluorescence Data Analysis. Fluorescence was assumed to decay multiexponentially according to the formula

$$I(t) = \sum_i \alpha_i e^{-t/\tau_i} \quad (3)$$

where τ_i and α_i are fluorescence lifetimes and corresponding amplitudes, respectively. The intensity decay $I(t)$ was analyzed by a maximum entropy method for oversampled data (SVD-MEM) coded according to the method of Bryan (*36*). Typically, we used 150 lifetimes in the range from 20 ps to 20 ns, equidistantly spaced on the logarithmic scale. The program yielded a set of amplitudes α_i representing a lifetime distribution in the decay. The mean lifetime was calculated as

$$\tau_{mean} = \sum_i f_i \tau_i \quad (4)$$

where index i runs over all lifetime components and f_i represents an intensity fraction of the corresponding component:

$$f_i = \alpha_i\tau_i / \sum_i \alpha_i\tau_i \quad (5)$$

Mass Spectrometric Analysis. Samples were first separated by 12% SDS−PAGE, and excised protein bands were digested with trypsin endoprotease (Promega) directly in gel (*37*). Resulting peptide mixtures were extracted with 30% acetonitrile and 0.3% acetic acid and assessed with MALDI-TOF mass spectrometer BIFLEX (Bruker-Franzen, Bremen, Germany) equipped with a nitrogen laser (337 nm) and gridless delayed extraction ion source. The ion acceleration voltage was 19 kV, and the reflectron voltage was set to 20 kV. Positive charged spectra were calibrated internally using the monoisotopic $[M + H]^+$ ions of tyrosine hydroxylase regulatory domain peptides with known sequence. A saturated solution of α-cyano-4-hydroxycinnamic acid in a 50% MeCN/0.3% acetic acid mixture was used as a MALDI matrix. A sample (1 μL) was loaded on the target, and the droplet was allowed to dry at ambient temperature, overlaid with 1 μL of matrix solution, and allowed to cocrystallize at ambient temperature, too. To enrich phosphorylated peptides from the peptide mixtures for postsource decay (PSD) analysis, the previously described procedure was used (*38*).

Native TBE−PAGE Analysis of Binding of TH1R to the 14-3-3ζ Protein. Phosphorylated TH1R (11.5 μM) was incubated with the 14-3-3ζ protein (0−27.5 μM) in buffer containing 20 mM Tris-HCl (pH 7.5), 150 mM NaCl, 1 mM EDTA, and 2 mM DTT for 15 min at 0 °C. The samples were then subjected to a native 15% TBE−PAGE. The binding of the dpTH1R to the 14-3-3ζ protein was quantified by a densitometric analysis of the resulting gel using ImageJ version 1.33u (*39*). The fraction of bound TH1R (F_B) was calculated from the formula

$$F_B = (I_{obs} - I_{min})/(I_{max} - I_{min}) \quad (6)$$

where the parameter I_{max} is the intensity of the TH1R−14-3-3ζ complex band at saturation, I_{obs} is the intensity of the complex band for any 14-3-3ζ protein concentration, and I_{min} is the minimum observed intensity of the complex band. F_B was plotted against the 14-3-3ζ protein concentration and fitted using eq 7 to estimate an apparent K_D for formation of the TH1R−14-3-3ζ complex (assuming 1:1 molar stoichiometry of the complex)

$$F_B = [K_D + [P1] + [P2] - \sqrt{(K_D + [P1] + [P2])^2 - 4[P1][P2]}]/2[P1] \quad (7)$$

where K_D is the equilibrium dissociation constant, [P1] is the TH1R concentration, and [P2] is the 14-3-3ζ protein concentration. Nonlinear data fitting was performed using Origin version 7.5 (Microcal Software Inc.).

RESULTS

Preparation of the Phosphorylated TH1R and Characterization of Its Interactions with 14-3-3ζ Protein. It has been suggested that the TH1R contains two potential 14-3-3 protein binding motifs around residues Ser^{19} and Ser^{40} (Figure 1A) (*16*−*19*, *25*). First, we tested whether the human 14-3-3ζ protein binds to the human TH1R phosphorylated only at Ser^{40} using native TBE−PAGE. These experiments, however, revealed that TH1R phosphorylated only at Ser^{40} does not interact with 14-3-3ζ protein. A similar negative result was also obtained for TH1R phosphorylated at Ser^{40} and containing mutation Ser^{19}Asp to mimic the negative charge of phosphorylated Ser^{19} (data not shown).

Residue Ser^{19} is known to be phosphorylated by Ca^{2+}/calmodulin-dependent kinase II (CAM-K2), mitogen-activated protein kinase-activated protein kinase 2 (*28*, *40*), or p38 regulated/activated kinase (*26*). Although CAM-K2 is commercially available, the preparation of milligram quantities of TH1R stoichiometrically phosphorylated at Ser^{19} turned out to be very difficult mainly due to the relatively low activity of CAM-K2. To prepare a larger quantity of the TH1R stoichiometrically phosphorylated at both Ser^{19} and Ser^{40} (denoted dpTH1R), residue Ala^{17} was mutated to Arg, thus making residue Ser^{19} a substrate for PKA. This protein was expressed, purified, and phosphorylated by PKA, and the result of the phosphorylation reaction was determined using MALDI-TOF mass spectrometry. Positive ion mass spectra were measured in the reflection mode to check the amino acid sequences of TH1R tryptic peptides. The comparison of positive MALDI-TOF mass spectra of digested unphosphorylated and phosphorylated samples clearly demonstrates two phosphorylated peptides in the sample of dpTH1R. The detected peaks in positive ion mass spectra of dpTH1R correspond to the phosphorylated peptide RVpS^{19}ELDAK having a protonized mass of *m*/*z* 997.5 (pS denotes phosphorylated Ser residue), the peptide with the sequence RQpS^{40}LIEDAR (having a mass of *m*/*z* 1167.5), or the peptide with the sequence RQpS^{40}LIEDARK having a mass of *m*/*z* 1295.5. No unphosphorylated moiety was identified in positive or negative mass spectra of the dpTH1R tryptic peptide map. On the other hand, the unphosphorylated TH1R mass spectrum provided only unphosphorylated peptides, and no peaks with the same *m*/*z* value as described for dpTH1R were detected. These results indicate that PKA-induced phosphorylation of Ser^{19} and Ser^{40} was stoichiometric. The identity and structure of both phosphorylated peptides were further corroborated by analysis of their positive PSD spectra after specific phosphopeptide enrichment to authenticate Ser^{19} and Ser^{40} as phosphorylated amino acids (data not shown).

A nondenaturing PAGE analysis was used to estimate an apparent equilibrium dissociation constant of the dpTH1R−14-3-3ζ protein complex. Samples of dpTH1R were incubated with different concentrations of 14-3-3ζ protein, and formation of the complex was monitored using native TBE−PAGE (Figure 2). The formation of the dpTH1R−14-3-3ζ complex was quantified by densitometric analysis, and the K_D of ∼421 ± 75 nM was estimated by fitting the resulting curve (assuming a 1:1 molar stoichiometry of the dpTH1R−14-3-3ζ complex). This binding affinity is comparable to that reported for the interaction between full-length TH1 and 14-3-3ζ protein (100−400 nM) (*25*).

Binding of 14-3-3ζ Protein Affects the Conformation of the N-Terminal Part of TH1R. To investigate the effect of 14-3-3ζ protein binding on the conformation of the TH1R, we performed time-resolved tryptophan fluorescence intensity measurements of single tryptophan residues inserted at five different positions within the TH1R molecule (Trp^{14}, Trp^{31}, Trp^{73}, Trp^{103}, and Trp^{131}). The sequence of the TH1R does not contain any tryptophan residue; thus, phenylalanines

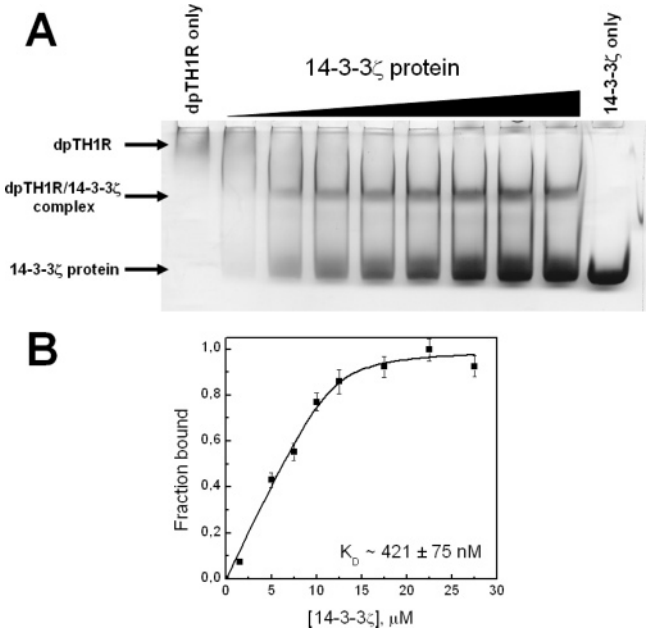

FIGURE 2: Nondenaturing TBE−PAGE analysis used to estimate the apparent equilibrium dissociation constant of the dpTH1R−14-3-3ζ protein complex. Samples of the dpTH1R were incubated with different concentrations of 14-3-3ζ protein, and the binding of dpTH1R to the 14-3-3ζ protein was monitored using native TBE−PAGE (A). Formation of the complex was quantified by densitometric analysis, and the K_D of ~421 ± 75 nM for binding of the dpTH1R to the 14-3-3ζ protein was estimated by fitting the resulting curve (B).

located at these positions were replaced with tryptophans. Time-resolved fluorescence intensity decays were analyzed using a singular-value decomposition maximum entropy method as described previously (*33*). The intensity decays of all five single-tryptophan TH1R mutants can be adequately described by a lifetime distribution containing three lifetime components. As an example, Figures 3 and 4 show the effect of phosphorylation and binding of the 14-3-3ζnoW protein on the fluorescence intensity decay and the fluorescence lifetime distribution of the TH1R containing tryptophan at position 34. The human 14-3-3ζnoW protein mutant missing all Trp residues (mutations Trp^{59}Phe and Trp^{228}Phe) was used in all TH1R tryptophan measurements. We have previously shown that these two mutations have no effect on binding properties of 14-3-3ζ protein (*33*, *41*). It can be noticed that phosphorylation at Ser^{19} and Ser^{40} has no effect on the fluorescence of Trp^{34}, while 14-3-3ζnoW protein binding causes a significant increase in mean excited-state lifetime (Figures 3C,D and 4A,B). All mean excited-state lifetimes (τ_{mean}) of both unphosphorylated and doubly phosphorylated single-tryptophan TH1R mutants in the absence and presence of 14-3-3ζnoW protein are listed in Table 1. It can be noticed that phosphorylation of TH1R at Ser^{19} and Ser^{40} by itself causes either no or only a small change in the τ_{mean} values of studied tryptophans, indicating limited phosphorylation-induced structural changes in the vicinity of these residues. On the other hand, the binding of the 14-3-3ζnoW protein causes a significant increase in τ_{mean} values of tryptophans at positions 14, 34, and 73. The increase in the mean fluorescence lifetime was most prominent in the case of the tryptophan residue located at position 73 (a 40% increase from 3.0 to 4.2 ns). The observed increase in the τ_{mean} values of Trp^{14}, Trp^{34}, and Trp^{73} could reflect the 14-3-3ζnoW protein-induced conformational change in the TH1R that affects interactions of these tryptophans with their surroundings. However, the observed changes could also be caused by a direct interaction of the 14-3-3ζnoW protein with these residues, thus changing their contacts with the polar environment or altering quenching interactions in their vicinity.

To examine the possible effect of shielding, we studied changes in the accessibility of all five tryptophan residues upon binding of the 14-3-3ζnoW protein by acrylamide quenching experiments in the absence and presence of the 14-3-3ζnoW protein. Results of the collisional quenching (Stern−Volmer or K_{SV} values) are listed in Table 2. The contribution of the static quenching, represented by a constant V in eq 1, in all cases was negligible (V was equal or very close to zero). Bimolecular quenching constants k_q, reflecting the accessibility of the fluorophore to the quencher, were then calculated from the ratio of the Stern−Volmer quenching constant K_{SV} and the mean fluorescence excited-state lifetime τ_{mean}. Figure 5 shows examples of Stern−Volmer plots for TH1R mutants containing Trp^{14}, Trp^{34}, and Trp^{73}. It is seen that for the TH1R mutants containing Trp^{14} and Trp^{34} the K_{SV} decreases upon binding of the 14-3-3ζ protein. For the Trp^{73} mutants, we observed an opposite effect. A significant decrease in the bimolecular quenching constant in the case of Trp^{14} and Trp^{34} (Table 2) clearly shows that accessibility of these tryptophan residues to the acrylamide significantly decreases in the TH1R−14-3-3ζnoW complex. Importantly, the accessibility of Trp^{73} to the solvent remains unaltered. Therefore, we can conclude that the observed increase in τ_{mean} cannot be caused by a simple steric shielding of Trp^{73} upon binding of the 14-3-3ζnoW protein. The solvent exposure of tryptophan residues at positions 73, 103, and 131 was found to remain practically unchanged in the TH1R−14-3-3ζnoW complex. At room temperature, the acrylamide bimolecular quenching constant of free Trp in solution is $\sim 5.9 \times 10^9$ M^{-1} s^{-1} (*42*). Comparison of this value with values in Table 2 indicates that all Trp residues are at least partially buried in the protein with rather restricted solvent accessibilities. Changes in τ_{mean} caused by a direct contact with 14-3-3ζnoW can therefore be excluded with high probability. At this moment, we cannot determine with certainty the extent to which the change in τ_{mean} and k_q observed in Trp^{14} and Trp^{34} mutants results from a conformational change in the N-terminal region (the region of the first 40 amino acid residues) and what could be a contribution of the steric shielding caused by the 14-3-3ζnoW protein binding. However, our results clearly indicate that the region of TH1R around Trp^{73} undergoes a 14-3-3 protein binding-induced structural change.

Circular Dichroism Measurements of TH1R. We then asked whether the 14-3-3ζ protein-induced conformational change in the TH1R observed by fluorescence spectroscopy could also be detected by circular dichroism. However, these experiments revealed that neither phosphorylation nor 14-3-3ζ protein binding induces any significant CD spectral change in the TH1R. The obtained far-UV CD spectra of the human TH1R (data not shown) were similar to those previously published for the regulatory domain of rat tyrosine hydroxylase (*4*). Deconvolution of our CD spectra revealed that the TH1R is an unstructured protein containing a large amount of random coil structure. Three deconvolution programs, including CONTIN/LL, SELCON3, and CDSSTR,

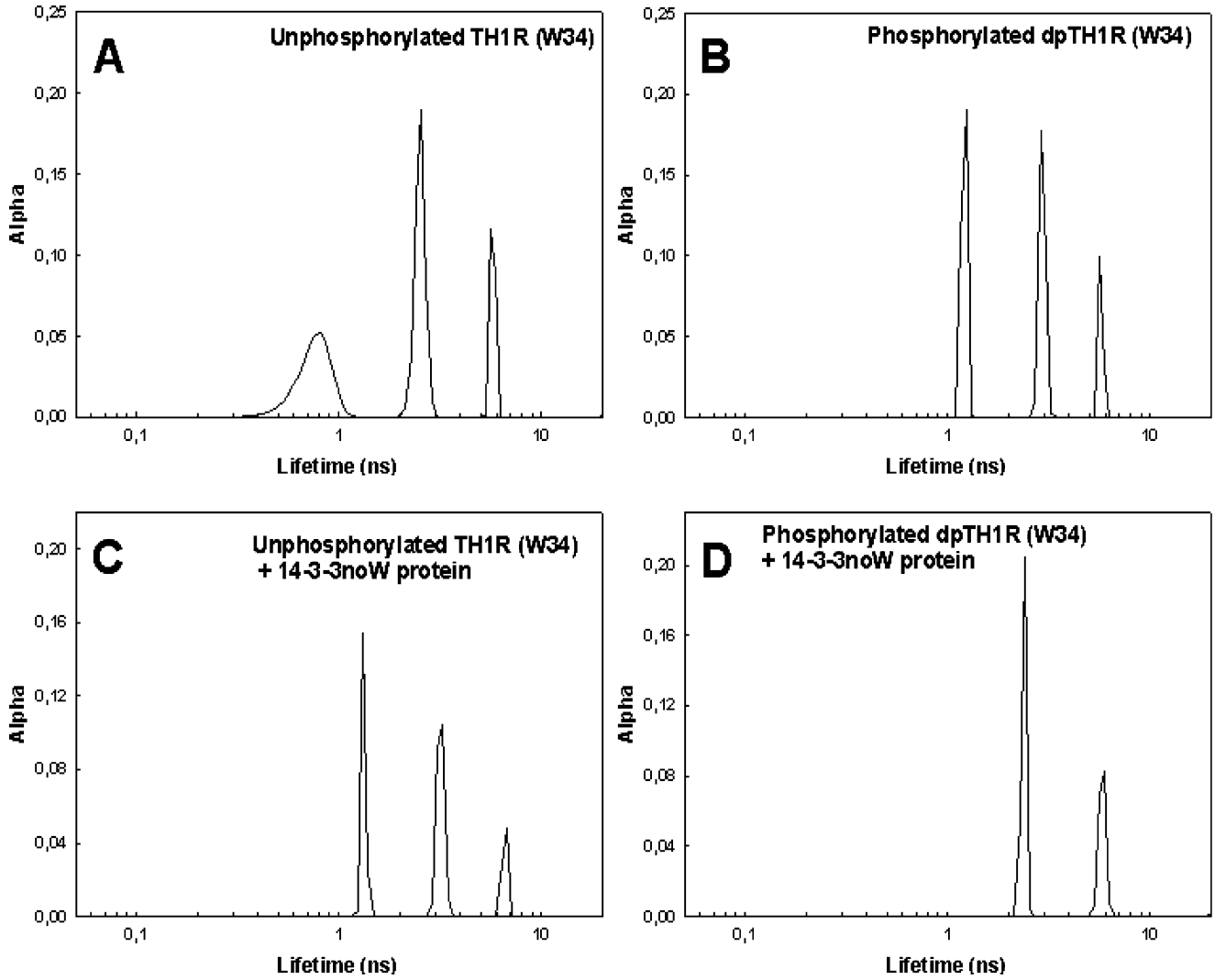

FIGURE 3: Excited-state lifetime distributions of TH1R containing Trp^{34}. (A) Unphosphorylated TH1R. (B) Doubly phosphorylated dpTH1R. (C) Unphosphorylated TH1R in the presence of the 14-3-3ζnoW protein. (D) Doubly phosphorylated dpTH1R in the presence of the 14-3-3ζnoW protein. The emission of tryptophan fluorescence was collected at 355 nm with excitation at 295 nm and room temperature. The human 14-3-3ζnoW protein mutant contains no Trp residue (mutations Trp^{59}Phe and Trp^{228}Phe) (*33*, *41*).

Table 1: Effect of Phosphorylation and Binding of the 14-3-3ζnoW Protein on Fluorescence Excited-State Lifetimes of Single-Tryptophan Mutants of TH1R

	mean fluorescence excited-state lifetime τ_{mean} (ns)[a]			
TH1R mutation	unphoshorylated TH1R	unphosphorylated TH1R with 14-3-3ζnoW	phosphorylated dpTH1R	phosphorylated dpTH1R with 14-3-3ζnoW
Trp^{14}	4.1	4.5	4.1	5.1
Trp^{34}	4.0	4.0	3.7	4.8
Trp^{73}	3.2	3.5	3.0	4.2
Trp^{103}	4.2	4.5	4.5	4.8
Trp^{131}	4.2	4.4	4.4	4.4

[a] The standard deviation is 0.05 ns.

were used to estimate secondary structure (*43*). All three methods gave similar results, but CDSSTR gave the best fit to the data. The average values for secondary structure composition of unphosphorylated TH1R from CDSSTR analysis were 30% β-sheet, 18% β-turn, 7% α-helix, and 45% unordered structure. This is in agreement with the theoretical prediction of disordered regions in TH1R using both loops/coils and hot-loops definitions (*44*−*46*) (Figure 1B).

Binding of 14-3-3ζ Protein Protects the TH1R against Proteolytic Degradation by Trypsin. It has been shown that the regulatory domain of tyrosine hydroxylase is very sensitive to proteolytic degradation mainly in the region between residues 33 and 50 (*12*). One of the suggested functions of the binding of 14-3-3 protein to TH is the structural stabilization of the enzyme. Since our fluorescence experiments revealed that the binding of 14-3-3ζ protein affects the conformation of the TH1R, we then asked whether

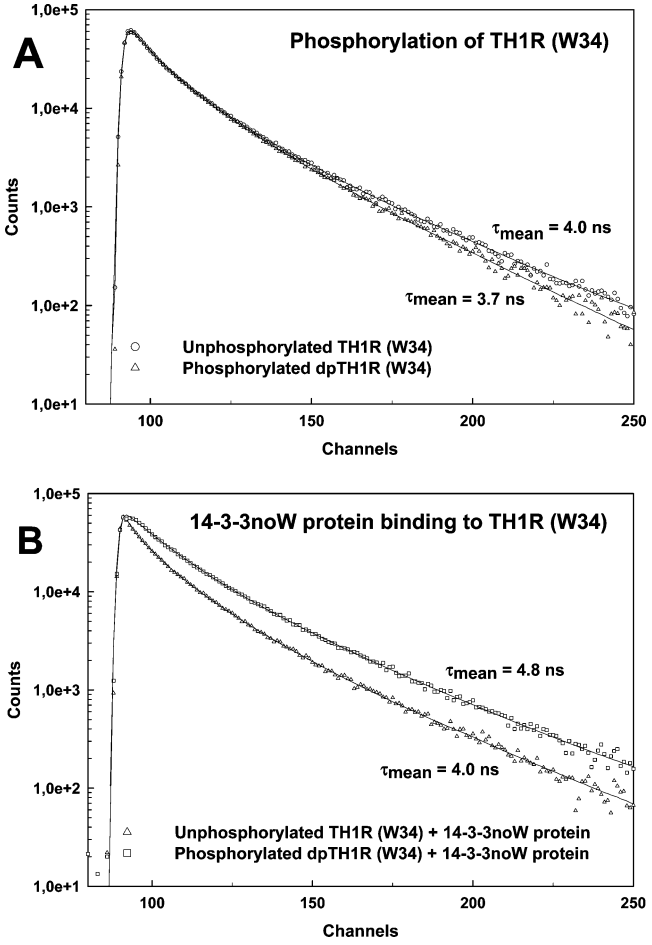

FIGURE 4: Fluorescence intensity decays of the TH1R containing Trp^{34}. (A) Comparison of fluorescence decays of the unphosphorylated TH1R and doubly phosphorylated dpTH1R. (B) Comparison of fluorescence decays of the unphosphorylated TH1R and doubly phosphorylated dpTH1R in the presence of the 14-3-3ζnoW protein. The time scale is 100 ps/channel.

the 14-3-3ζ protein is able to slow the proteolysis of the TH1R. Figure 6A shows results of the limited proteolysis of TH1R, dpTH1R, and 14-3-3ζ protein by low levels of trypsin (0.02%, w/w). It can be noticed that under conditions used in this experiment both unphosphorylated and phosphorylated TH1R were very sensitive to proteolysis, and in both cases, the cleavage resulted in the formation of a fragment with an apparent M_r of 15 000. The 14-3-3ζ protein was resistant to trypsin within the time course of this experiment. Results of limited proteolysis of TH1R−14-3-3ζ complexes are presented in Figure 6B. The 14-3-3ζ protein binding significantly slowed the cleavage of the phosphorylated dpTH1R compared to that of the dpTH1R alone (compare panels A and B of Figure 6). MALDI-TOF mass spectra were then used to identify the dominant cleavage site which generates a fragment of the TH1R with an apparent M_r of 15 000. All these SDS−PAGE bands from Figure 6 were further trypsinized, and positive ion mass spectra of resulting peptide mixtures were measured in the reflection mode to determine the amino acid sequences of tryptic peptides. The comparison of positive MALDI-TOF mass spectra with theoretical peptide maps resulted in a sequence coverage from Phe^{34} to the C-terminal end (Ser^{157}) in all analyzed samples. This corresponds to a theoretical mass of 13 655 Da of the intact protein after the partial trypsin digest. The phosphorylation of Ser^{40} was detected in the analyzed fragment of the doubly phoshorylated dpTH1R similarly as shown above.

DISCUSSION

Tyrosine hydroxylase, and phenylalanine hydroxylase and tryptophan hydroxylase, are metalloproteins that catalyze ring hydroxylation of aromatic amino acids while using tetrahydrobiopterin as the reducing substrate (*47*, *48*). All three enzymes consist of three domains: N-terminal regulatory domain, catalytic domain, and C-terminal tetramerization segment. While catalytic domains of these enzymes are homologous, the sequences of their regulatory domains differ substantially. Regulation of TH enzyme activity is linked with the posttranslational modification of its regulatory domain (*6*−*9*, *11*, *13*, *49*, *50*). TH activation by phosphorylation of its regulatory domain is the main mechanism responsible for the maintenance of catecholamine levels in tissues after their secretion. The regulatory domain of TH can be phosphorylated at four sites by a variety of protein kinases. The consequences of the phosphorylation have been extensively studied, and the best understood are the effects of the phosphorylation of residue Ser^{40}. Modification of this serine by PKA relieves the enzyme from the feedback inhibition by dopamine and DOPA (*8*, *9*, *11*, *15*, *49*). For the other sites, the effect of phosphorylation has not yet been fully established.

Phosphorylation of Ser^{19} by CaMKII or p38 regulated/activated kinase does not by itself increase TH activity but induces binding of the regulatory 14-3-3 protein (*17*, *18*, *25*, *26*, *28*, *51*). The role of the 14-3-3 protein binding in the regulation of TH activity is still not fully understood. It has been shown that the interaction of 14-3-3 protein with TH phosphorylated at Ser^{19} increases its activity and decreases the rate of Ser^{19} and Ser^{40} dephosphorylation. However, the mechanisms of these processes are unknown.

Table 2: Acrylamide Quenching Parameters for Single-Tryptophan Mutants of TH1R

sample	K_{SV} (M^{-1})	τ_{mean} (ns)	k_q ($\times 10^{-9}$ M^{-1} s^{-1})	λ_{max}[a] (nm)
TH1R(Trp^{14}) with 14-3-3ζnoW	7.37 ± 0.06	4.5	1.64 ± 0.01	348
dpTH1R(Trp^{14}) with 14-3-3ζnoW	5.77 ± 0.39	5.1	1.13 ± 0.08	345
TH1R(Trp^{34}) with 14-3-3ζnoW	6.88 ± 0.11	4.0	1.72 ± 0.03	346
dpTH1R(Trp^{34}) with 14-3-3ζnoW	4.82 ± 0.91	4.8	1.00 ± 0.19	344
TH1R(Trp^{73}) with 14-3-3ζnoW	4.56 ± 0.06	3.5	1.30 ± 0.02	340
dpTH1R(Trp^{73}) with 14-3-3ζnoW	5.32 ± 0.03	4.2	1.27 ± 0.01	338
TH1R(Trp^{103}) with 14-3-3ζnoW	4.44 ± 0.12	4.5	0.98 ± 0.03	349
dpTH1R(Trp^{103}) with 14-3-3ζnoW	5.08 ± 0.15	4.8	1.05 ± 0.03	349
TH1R(Trp^{131}) with 14-3-3ζnoW	5.30 ± 0.14	4.4	1.20 ± 0.03	350
dpTH1R(Trp^{131}) with 14-3-3ζnoW	5.12 ± 0.17	4.4	1.16 ± 0.04	351

[a] Maxima of fluorescence emission spectra.

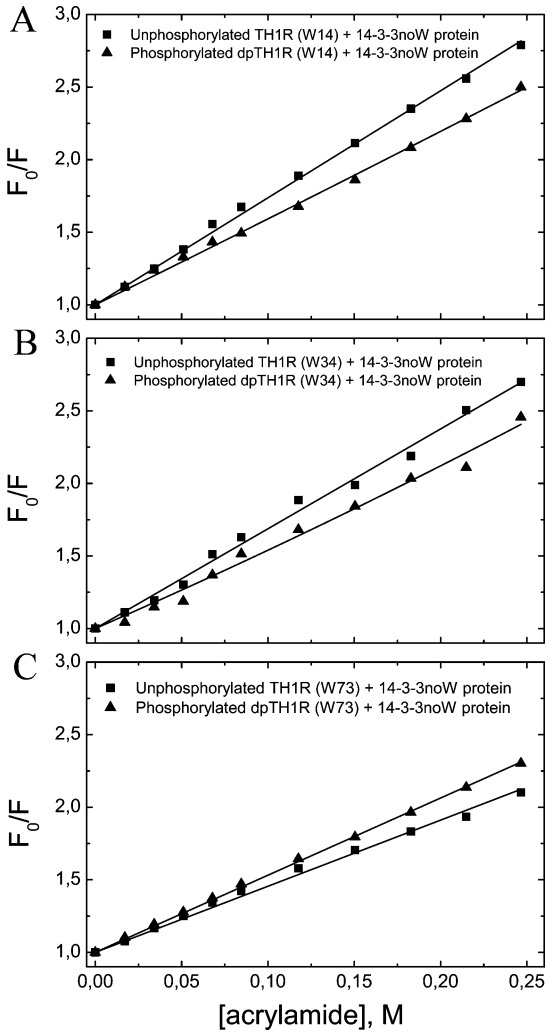

FIGURE 5: Stern−Volmer plots of collisional quenching of TH1R mutants containing Trp^{14} (A), Trp^{34} (B), and Trp^{73} (C). The results of data analysis are presented as the collisional quenching (Stern−Volmer) constant (K_{SV}) as listed in Table 2. The contribution of the static quenching, represented by a constant V in eq 1, was in all cases negligible (V was equal or very close to zero). The bimolecular quenching constant was then calculated from the ratio of the Stern−Volmer quenching constant K_{SV} to the mean fluorescence excited-state lifetime τ_{mean}.

In this work, we investigated whether the 14-3-3ζ protein binding affects the conformation of the regulatory domain of human TH (isoform 1). To study conformational changes of the TH1R, we prepared five mutants of the TH1R containing a single tryptophan residue at different positions within the domain (14, 34, 73, 103, and 131). To ensure the stoichiometric phosphorylation of the TH1R at both Ser^{19} and Ser^{40}, we mutated residue Ala^{17} to Arg to make Ser^{19}, along with Ser^{40}, a target for PKA. MALDI-TOF mass spectrometry measurements revealed that the TH1R Ala^{17}-Arg mutant is phosphorylated by PKA stoichiometrically at both serine residues. Results of tryptophan fluorescence measurements clearly indicate that the 14-3-3ζ protein directly interacts with the N-terminal half of the TH1R (region of the first 80 amino acid residues) as documented by an increase in τ_{mean} of tryptophans at positions 14, 34, and 73 (Table 1 and Figures 3 and 4). The increase in τ_{mean} indicates a significant change in quenching interactions in the vicinity of tryptophan residues (*35*, *52*). This could originate from two different processes: (i) the 14-3-3ζnoW protein-induced conformational change in the TH1R and (ii) a direct interaction of the 14-3-3ζnoW protein with these tryptophan residues that shields them from contacts with polar solvent (*52*). To distinguish between these two processes we studied changes in the accessibility of all five tryptophan residues upon the 14-3-3ζnoW protein binding by acrylamide quenching. These experiments revealed that all studied Trp residues are at least partially buried in the protein with rather restricted solvent accessibilities. The accessibility of Trp^{14} and Trp^{34} to the acrylamide significantly decreases in the dpTH1R−14-3-3ζnoW complex, while the accessibility of the Trp^{73} to the solvent remains unaltered (Table 2). Taken together, these results indicate that the observed increase in the τ_{mean} of Trp^{73} cannot be caused just by simple steric shielding from contacts with polar solvent but rather reflects the 14-3-3ζnoW protein-induced structural change in the dpTH1R in the region surrounding Trp^{73}. As far as Trp^{14} and Trp^{34} mutants are concerned, we cannot determine with certainty the extent to which the change in τ_{mean} and k_q observed in Trp^{14} and Trp^{34} mutants results from the conformational change in the dpTH1R and what could be a contribution of the steric shielding from the solvent caused by the 14-3-3ζnoW protein binding. The rest of the regulatory domain (regions around Trp^{103} and Trp^{131}) seems to be unaffected by the binding of the 14-3-3ζnoW protein. Phosphorylation of Ser^{19} and Ser^{40} by itself had no significant effect on the τ_{mean} values of all studied tryptophans, indicating no or little structural change in the vicinity of these residues (Table 1). However, it has been previously suggested that phosphorylation at Ser^{19} and Ser^{40} induces a conformational change in TH (*12*, *13*, *29*, *50*, *53*). Therefore, it seems that this phosphorylation-induced conformational change affects

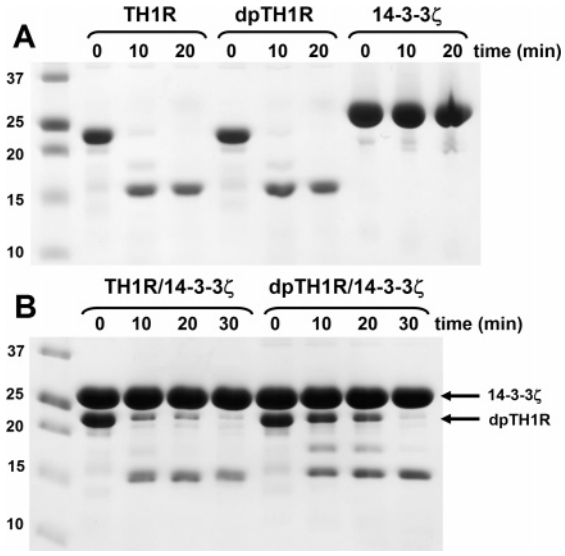

FIGURE 6: Limited proteolysis of the TH1R, dpTH1R, and 14-3-3ζ protein. (A) Limited proteolysis of the unphosphorylated TH1R, doubly phosphorylated dpTH1R, and 14-3-3ζ protein alone. The concentration of trypsin was 0.02% (w/w). (B) Limited proteolysis of TH1R−14-3-3ζ and dpTH1R−14-3-3ζ complexes. In the presence of the 14-3-3ζ protein, the cleavage of the phosphorylated dpTH1R is significantly slowed compared to that of the dpTH1R alone (compare panels A and B). Samples were incubated with trypsin for 10, 20, or 30 min at room temperature in buffer containing 20 mM Tris-HCl (pH 7.5), 150 mM NaCl, 2 mM 2-mercaptoethanol, and 10% (w/v) glycerol. The reaction was stopped with phenylmethanesulfonyl fluoride, and samples were resolved via 15% SDS−PAGE.

the regulatory domain in regions that are not in the vicinity of tryptophan residues used in this study.

Circular dichroism measurements revealed that the structural changes induced by both phosphorylation and the 14-3-3 protein do not affect the overall secondary structure of the TH1R. Deconvolution of the measured CD spectra suggests that the TH1R contains a large amount (~45%) of unstructured regions, in good agreement with the theoretical prediction (Figure 1B). High disorder can explain the known high sensitivity of the TH1R toward proteolytic degradation. It has been shown that the region from residue 33 to 50 is highly sensitive to mild trypsin digestion (*12*). We have observed that binding of the 14-3-3ζ protein decreases the rate of tryptic degradation of the dpTH1R in this region (Figure 6), suggesting that one of the roles of 14-3-3 protein might be the protection of the regulatory domain against proteolytic degradation. We may speculate that alteration of the sensitivity of the dpTH1R to proteolysis could also be the result of a 14-3-3 protein-induced conformational change in the dpTH1R in the vicinity of trypsin cleavage sites. The most prominent trypsin cleavage site of TH1R is located between residues 33 and 34 as identified by MALDI-TOF mass spectrometry. This is one of the regions affected by the 14-3-3ζnoW protein binding as documented by changes in τ_{mean} and k_q of Trp^{34} (Tables 1 and 2 and Figure 3).

It has been shown that more that 90% of known 14-3-3 protein binding partners contain disordered regions (*54*). Almost all 14-3-3 binding sites are located inside of these disordered regions (*54*). Therefore, a hypothesis that 14-3-3 protein binding induces a disorder-to-order transition was proposed. On the basis of our results, it is possible to speculate that the regulatory domain of TH is an example of such a disordered protein. The binding of 14-3-3 protein to the TH1R alters its conformation, increases its stability, and slows dephosphorylation of Ser^{40}, thus helping to keep TH in the activated state.

In conclusion, we have studied interaction of the doubly phosphorylated TH1R with the 14-3-3ζ protein. Site-directed mutagenesis was used to generate five single-tryptophan mutants with the Trp residue located at five different positions within the regulatory domain (positions 14, 34, 73, 103, and 131). Time-resolved tryptophan fluorescence measurements revealed that phosphorylation of Ser^{19} and Ser^{40} by itself does not induce any significant conformational change in regions surrounding inserted tryptophans. On the other hand, the interaction between the 14-3-3 protein and the phosphorylated TH1R decreases the solvent exposure of tryptophan residues at positions 14 and 34 and induces a distinct structural change in the vicinity of Trp^{73}. The 14-3-3ζ protein binding also reduces the sensitivity of the dpTH1R to proteolysis by protecting its N-terminal part (first 33 residues). Circular dichroism measurements showed that the regulatory domain of TH is an unstructured protein with a low content of secondary structure and that neither phosphorylation nor 14-3-3ζ protein binding changes its secondary structure.

ACKNOWLEDGMENT

We thank Dr. S. C. Daubner for providing us with the cDNA clone of human TH1R.

REFERENCES

1. Nagatsu, T., Levitt, M., and Udenfriend, S. (1964) Tyrosine Hydroxylase. The Initial Step in Norepinephrine Biosynthesis, *J. Biol. Chem. 239*, 2910−2917.
2. Kumer, S. C., and Vrana, K. E. (1996) Intricate regulation of tyrosine hydroxylase activity and gene expression, *J. Neurochem. 67*, 443−462.
3. Fitzpatrick, P. F. (1999) Tetrahydropterin-dependent amino acid hydroxylases, *Annu. Rev. Biochem. 68*, 355−381.
4. Daubner, S. C., Lohse, D. L., and Fitzpatrick, P. F. (1993) Expression and characterization of catalytic and regulatory domains of rat tyrosine hydroxylase, *Protein Sci. 2*, 1452−1460.
5. Haycock, J. W. (1990) Phosphorylation of tyrosine hydroxylase in situ at serine 8, 19, 31, and 40, *J. Biol. Chem. 265*, 11682−11691.
6. Haycock, J. W., and Haycock, D. A. (1991) Tyrosine hydroxylase in rat brain dopaminergic nerve terminals. Multiple-site phosphorylation in vivo and in synaptosomes, *J. Biol. Chem. 266*, 5650−5657.
7. Dunkley, P. R., Bobrovskaya, L., Graham, M. E., von Nagy-Felsobuki, E. I., and Dickson, P. W. (2004) Tyrosine hydroxylase phosphorylation: Regulation and consequences, *J. Neurochem. 91*, 1025−1043.
8. Ramsey, A. J., and Fitzpatrick, P. F. (1998) Effects of phosphorylation of serine 40 of tyrosine hydroxylase on binding of catecholamines: Evidence for a novel regulatory mechanism, *Biochemistry 37*, 8980−8986.
9. Daubner, S. C., Lauriano, C., Haycock, J. W., and Fitzpatrick, P. F. (1992) Site-directed mutagenesis of serine 40 of rat tyrosine hydroxylase. Effects of dopamine and cAMP-dependent phosphorylation on enzyme activity, *J. Biol. Chem. 267*, 12639−12646.
10. Ribeiro, P., Wang, Y., Citron, B. A., and Kaufman, S. (1992) Regulation of recombinant rat tyrosine hydroxylase by dopamine, *Proc. Natl. Acad. Sci. U.S.A. 89*, 9593−9597.
11. Wu, J., Filer, D., Friedhoff, A. J., and Goldstein, M. (1992) Site-directed mutagenesis of tyrosine hydroxylase. Role of serine 40 in catalysis, *J. Biol. Chem. 267*, 25754−25758.
12. McCulloch, R. I., and Fitzpatrick, P. F. (1999) Limited proteolysis of tyrosine hydroxylase identifies residues 33−50 as conformationally sensitive to phosphorylation state and dopamine binding, *Arch. Biochem. Biophys. 367*, 143−145.
13. Bevilaqua, L. R., Graham, M. E., Dunkley, P. R., von Nagy-Felsobuki, E. I., and Dickson, P. W. (2001) Phosphorylation of Ser(19) alters the conformation of tyrosine hydroxylase to increase the rate of phosphorylation of Ser(40), *J. Biol. Chem. 276*, 40411−40416.
14. McCulloch, R. I., Daubner, S. C., and Fitzpatrick, P. F. (2001) Effects of substitution at serine 40 of tyrosine hydroxylase on catecholamine binding, *Biochemistry 40*, 7273−7278.
15. Sura, G. R., Daubner, S. C., and Fitzpatrick, P. F. (2004) Effects of phosphorylation by protein kinase A on binding of catecholamines to the human tyrosine hydroxylase isoforms, *J. Neurochem. 90*, 970−978.
16. Yamauchi, T., and Fujisawa, H. (1981) Tyrosine 3-monoxygenase is phosphorylated by Ca^{2+}-, calmodulin-dependent protein kinase, followed by activation by activator protein, *Biochem. Biophys. Res. Commun. 100*, 807−813.
17. Yamauchi, T., Nakata, H., and Fujisawa, H. (1981) A new activator protein that activates tryptophan 5-monooxygenase and tyrosine 3-monooxygenase in the presence of Ca^{2+}-, calmodulin-dependent protein kinase. Purification and characterization, *J. Biol. Chem. 256*, 5404−5409.
18. Ichimura, T., Isobe, T., Okuyama, T., Yamauchi, T., and Fujisawa, H. (1987) Brain 14-3-3 protein is an activator protein that activates tryptophan 5-monooxygenase and tyrosine 3-monooxygenase in the presence of Ca^{2+}, calmodulin-dependent protein kinase II, *FEBS Lett. 219*, 79−82.
19. Itagaki, C., Isobe, T., Taoka, M., Natsume, T., Nomura, N., Horigome, T., Omata, S., Ichinose, H., Nagatsu, T., Greene, L. A., and Ichimura, T. (1999) Stimulus-coupled interaction of tyrosine hydroxylase with 14-3-3 proteins, *Biochemistry 38*, 15673−15680.
20. Fu, H., Subramanian, R. R., and Masters, S. C. (2000) 14-3-3 proteins: Structure, function, and regulation, *Annu. Rev. Pharmacol. Toxicol. 40*, 617−647.
21. Aitken, A. (2006) 14-3-3 proteins: A historic overview, *Semin. Cancer Biol. 16*, 162−172.

22. Muslin, A. J., Tanner, J. W., Allen, P. M., and Shaw, A. S. (1996) Interaction of 14-3-3 with signaling proteins is mediated by the recognition of phosphoserine, *Cell 84*, 889−897.
23. Yaffe, M. B., Rittinger, K., Volinia, S., Caron, P. R., Aitken, A., Leffers, H., Gamblin, S. J., Smerdon, S. J., and Cantley, L. C. (1997) The structural basis for 14-3-3:phosphopeptide binding specificity, *Cell 91*, 961−971.
24. Rittinger, K., Budman, J., Xu, J., Volinia, S., Cantley, L. C., Smerdon, S. J., Gamblin, S. J., and Yaffe, M. B. (1999) Structural analysis of 14-3-3 phosphopeptide complexes identifies a dual role for the nuclear export signal of 14-3-3 in ligand binding, *Mol. Cell 4*, 153−166.
25. Kleppe, R., Toska, K., and Haavik, J. (2001) Interaction of phosphorylated tyrosine hydroxylase with 14-3-3 proteins: Evidence for a phosphoserine 40-dependent association, *J. Neurochem. 77*, 1097−1107.
26. Toska, K., Kleppe, R., Armstrong, C. G., Morrice, N. A., Cohen, P., and Haavik, J. (2002) Regulation of tyrosine hydroxylase by stress-activated protein kinases, *J. Neurochem. 83*, 775−783.
27. Haycock, J. W., and Wakade, A. R. (1992) Activation and multiple-site phosphorylation of tyrosine hydroxylase in perfused rat adrenal glands, *J. Neurochem. 58*, 57−64.
28. Sutherland, C., Alterio, J., Campbell, D. G., Le Bourdelles, B., Mallet, J., Haavik, J., and Cohen, P. (1993) Phosphorylation and activation of human tyrosine hydroxylase in vitro by mitogen-activated protein (MAP) kinase and MAP-kinase-activated kinases 1 and 2, *Eur. J. Biochem. 217*, 715−722.
29. Royo, M., Fitzpatrick, P. F., and Daubner, S. C. (2005) Mutation of regulatory serines of rat tyrosine hydroxylase to glutamate: Effects on enzyme stability and activity, *Arch. Biochem. Biophys. 434*, 266−274.
30. Obsil, T., Ghirlando, R., Klein, D. C., Ganguly, S., and Dyda, F. (2001) Crystal structure of the 14-3-3ζ:serotonin N-acetyltransferase complex. a role for scaffolding in enzyme regulation, *Cell 105*, 257−267.
31. Obsilova, V., Vecer, J., Herman, P., Pabianova, A., Sulc, M., Teisinger, J., Boura, E., and Obsil, T. (2005) 14-3-3 protein interacts with nuclear localization sequence of forkhead transcription factor FoxO4, *Biochemistry 44*, 11608−11617.
32. Yaffe, M. B. (2002) How do 14-3-3 proteins work? Gatekeeper phosphorylation and the molecular anvil hypothesis, *FEBS Lett. 513*, 53−57.
33. Obsilova, V., Herman, P., Vecer, J., Sulc, M., Teisinger, J., and Obsil, T. (2004) 14-3-3ζ C-terminal stretch changes its conformation upon ligand binding and phosphorylation at Thr232, *J. Biol. Chem. 279*, 4531−4540.
34. Eftink, M. R., and Ghiron, C. A. (1976) Exposure of Tryptophanyl Residues in Proteins: Quantitative Determination by Fluorescence Quenching Studies, *Biochemistry 15*, 672−680.
35. Lakowicz, J. R. (1983) *Principles of Fluorescence Spectroscopy*, Plenum Press, New York.
36. Bryan, R. K. (1990) Maximum-Entropy Analysis of Oversampled Data Problems. *Eur. Biophys. J. 18*, 165−174.
37. Kovarova, H., Halada, P., Man, P., Golovliov, I., Krocova, Z., Spacek, J., Porkertova, S., and Necasova, R. (2002) Proteome study of *Francisella tularensis* live vaccine strain-containing phagosome in Bcg/Nramp1 congenic macrophages: Resistant allele contributes to permissive environment and susceptibility to infection, *Proteomics 2*, 85−93.
38. Larsen, M. R., Thingholm, T. E., Jensen, O. N., Roepstorff, P., and Jorgensen, T. J. (2005) Highly selective enrichment of phosphorylated peptides from peptide mixtures using titanium dioxide microcolumns, *Mol. Cell. Proteomics 4*, 873−886.
39. Abramoff, M. D., Magelhaes, P. J., and Ram, S. J. (2004) Image Processing with ImageJ, *Biophotonics Int. 11*, 36−42.
40. Vulliet, P. R., Woodgett, J. R., and Cohen, P. (1984) Phosphorylation of tyrosine hydroxylase by calmodulin-dependent multiprotein kinase, *J. Biol. Chem. 259*, 13680−13683.
41. Silhan, J., Obsilova, V., Vecer, J., Herman, P., Sulc, M., Teisinger, J., and Obsil, T. (2004) 14-3-3 protein C-terminal stretch occupies ligand binding groove and is displaced by phosphopeptide binding, *J. Biol. Chem. 279*, 49113−49119.
42. Herman, P., Vecer, J., Scognamiglio, V., Staiano, M., Rossi, M., and D'Auria, S. (2004) A recombinant glutamine-binding protein from *Escherichia coli*: Effect of ligand-binding on protein conformational dynamics, *Biotechnol. Prog. 20*, 1847−1854.
43. Whitmore, L., and Wallace, B. A. (2004) DICHROWEB, an online server for protein secondary structure analyses from circular dichroism spectroscopic data, *Nucleic Acids Res. 32*, W668−W673.
44. Kabsch, W., and Sander, C. (1983) Dictionary of protein secondary structure: Pattern recognition of hydrogen-bonded and geometrical features, *Biopolymers 22*, 2577−2637.
45. Smith, D. K., Radivojac, P., Obradovic, Z., Dunker, A. K., and Zhu, G. (2003) Improved amino acid flexibility parameters, *Protein Sci. 12*, 1060−1072.
46. Linding, R., Jensen, L. J., Diella, F., Bork, P., Gibson, T. J., and Russell, R. B. (2003) Protein disorder prediction: Implications for structural proteomics, *Structure 11*, 1453−1459.
47. Kaufman, S. (1995) Tyrosine hydroxylase, *Adv. Enzymol. Relat. Areas Mol. Biol. 70*, 103−220.
48. Hufton, S. E., Jennings, I. G., and Cotton, R. G. (1995) Structure and function of the aromatic amino acid hydroxylases, *Biochem. J. 311* (Part 2), 353−366.
49. Almas, B., Le Bourdelles, B., Flatmark, T., Mallet, J., and Haavik, J. (1992) Regulation of recombinant human tyrosine hydroxylase isozymes by catecholamine binding and phosphorylation. Structure/activity studies and mechanistic implications, *Eur. J. Biochem. 209*, 249−255.
50. Martinez, A., Haavik, J., Flatmark, T., Arrondo, J. L., and Muga, A. (1996) Conformational properties and stability of tyrosine hydroxylase studied by infrared spectroscopy. Effect of iron/catecholamine binding and phosphorylation, *J. Biol. Chem. 271*, 19737−19742.
51. Haycock, J. W., Lew, J. Y., Garcia-Espana, A., Lee, K. Y., Harada, K., Meller, E., and Goldstein, M. (1998) Role of serine-19 phosphorylation in regulating tyrosine hydroxylase studied with site- and phosphospecific antibodies and site-directed mutagenesis, *J. Neurochem. 71*, 1670−1675.
52. Kirby, E. P., and Steiner, R. F. (1970) The influence of solvent and temperature upon the fluorescence of indole derivatives, *J. Phys. Chem. 74*, 4480−4490.
53. Gahn, L. G., and Roskoski, R., Jr. (1995) Thermal stability and CD analysis of rat tyrosine hydroxylase, *Biochemistry 34*, 252−256.
54. Bustos, D. M., and Iglesias, A. A. (2006) Intrinsic disorder is a key characteristic in partners that bind 14-3-3 proteins, *Proteins 63*, 35−42.

BI7019468